ceramics

MDPI

Article

Powder Mixture for the Production of Microporous Ceramics Based on Hydroxyapatite

Tatiana Safronova [1,2,*], Stepan Chichulin [1], Tatiana Shatalova [1,2] and Yaroslav Filippov [2,3]

[1] Department of Chemistry, Lomonosov Moscow State University, Building, 3, Leninskie Gory, 1, 119991 Moscow, Russia; chichulinsn@my.msu.ru (S.C.); shatalovatb@gmail.com (T.S.)
[2] Department of Materials Science, Lomonosov Moscow State University, Building, 73, Leninskie Gory, 1, 119991 Moscow, Russia; filippovyy@my.msu.ru
[3] Research Institute of Mechanics, Lomonosov Moscow State University, Michurinsky Pr., 1, 119192 Moscow, Russia
* Correspondence: safronovatv@my.msu.ru; Tel.: +7-916-3470-641

Abstract: Powder mixtures with a given molar ratio of Ca/P = 1.67 were prepared under mechanical activation conditions from hydroxyapatite powder $Ca_{10}(PO_4)_6(OH)_2$ and a 1M aqueous solution of oxalic acid $H_2C_2O_4$ at a molar ratio of $Ca_{10}(PO_4)_6(OH)_2/H_2C_2O_4$ = 1:4. The phase composition of obtained powder mixture included brushite (calcium hydrophosphate dihydrate) $CaHPO_4{\cdot}2H_2O$, calcium oxalate monohydrate $CaC_2O_4{\cdot}H_2O$ in form of whewellite and weddellite, and some quantity of quasi-amorphous phase. This powder mixture was used to produce microporous monophase ceramics based on hydroxyapatite $Ca_{10}(PO_4)_6(OH)_2$ with apparent density of 1.25 g/cm^3 after firing at 1200 °C. Microporosity of sintered ceramics was formed due to the presence of particles with plate-like morphology, restraining shrinkage during sintering. Microporous ceramics based on hydroxyapatite $Ca_{10}(PO_4)_6(OH)_2$ with the roughness of the surface as a consequence of the created microporosity can be recommended as a biocompatible material for bone defects treatment and as a substrate for bone cell cultivation.

Keywords: hydroxyapatite; oxalic acid; powder; whewellite; weddellite; calcium oxalate monohydrate; brushite; calcium hydrophosphate dihydrate; heterophase reaction; ceramics; microporosity

Citation: Safronova, T.; Chichulin, S.; Shatalova, T.; Filippov, Y. Powder Mixture for the Production of Microporous Ceramics Based on Hydroxyapatite. *Ceramics* **2022**, *5*, 108–119. https://doi.org/10.3390/ceramics5010010

Academic Editors: Margarita A. Goldberg, Elisa Torresani and Gilbert Fantozzi

Received: 31 January 2022
Accepted: 16 February 2022
Published: 18 February 2022

1. Introduction

The creation of ceramic materials based on calcium phosphates is one of the intensively developing areas of modern materials science for medicine [1]. These materials are biocompatible and can be used in medicine as porous matrices for replacing lost or damaged bone tissue or as substrates for cell cultivation. Ceramics based on hydroxyapatite $Ca_{10}(PO_4)_6(OH)_2$ (HA) are widely used as material for bone implants creation due to its stability and the similarity of chemical and phase compositions of inorganic part of natural bone [2,3].

Ceramics for bone implants have to be porous with at least two levels of porosity to mimic the natural bone. Macro pores have to be no less than 100 μm, and the dimension of micropores should be about 10 μm [4,5]. Microporosity of ceramics producing roughness on the surface can improve biointegration and osteoconductivity of material and ensure effective fixation and reproduction of bone tissue cells, as well as a fusion of the implant with the body [6].

Ceramics based on hydroxyapatite are very often prepared from HA powder previously synthesized by various methods. Among them, the following two big groups of methods should be noted: syntheses in the presence of water and anhydrous syntheses [7]. Aqueous syntheses include synthesis by precipitation from aqueous solutions [8], hydrolysis [9], hydrothermal synthesis [10], synthesis in aqueous suspensions and pastes [11].

Anhydrous syntheses include solid-phase synthesis [12,13], synthesis by fusion of oxides or salts [14], synthesis in molten salts [15], and synthesis in non-aqueous solvents [16]. Methods using aqueous or nonaqueous solutions and suspension can be carried out at additional impacts of microwave radiation [17], mechanical activation [18], ultrasound radiation [19], or combustion [20]. The simplest and most common method to obtain hydroxyapatite powder is its precipitation from an aqueous solution of the corresponding substances, which are phosphoric acid or soluble phosphates of ammonium, sodium, potassium as phosphate ion sources and soluble calcium salts (acetate, nitrate, and chloride) as calcium ion sources [21,22]. Another method to prepare HA powders or ceramics comprises heat treatment of preliminarily homogenized powder mixtures of different salts with the preset molar ratio of Ca/P = 1.67 [23]. As far as precipitation can realize the bottom-up approach, the obvious advantage of this method consists in the preparation of active powders with a small dimension and quite a large quantity of defects in the crystal structure. Disadvantages of the synthesis of calcium phosphates via precipitation comprise large sensitivity of phase composition of the resulting precipitate to the pH of the reaction zone. Solid-state synthesis using heat treatment of thoroughly homogenized powder mixtures provides better opportunities to prepare hydroxyapatite or another calcium phosphate with target molar ratio Ca/P. Of course, the mean dimension of particles of prepared powder can be larger than in powders prepared via precipitation. However, fine precipitated powders have a tendency to form quite large aggregates and additional actions for preventing aggregation before molding and sintering should be performed.

To create microporosity, one can use a special thermal treatment scheduler to obtain undersintered ceramic material [24] or via a sol-gel synthesis-prepared powder system [25]. Another method of microporosity creation consists in using organic [26,27] or inorganic [28,29] additives in form of particles with small dimensions as sacrificed porogens. Special additives that have the ability to decompose with the release of sufficiently large volumes of gases at different stages of ceramics production can be used to generate microporosity. CO_2 and NH_3 from NH_4CO_3 can be used, for example, at the stage of slurry preparation [30], or CO_2 from sodium or potassium carbonates in the presence of melt can be used at the stage of heat treatment [31] for the creation of the microporosity of materials.

In the present work for preparing of microporous HA-ceramics, we used an intentionally prepared powder mixture including particles with the plate-like morphology, expecting that particles with this form can restrain sintering.

The purpose of this work consisted in preparing and investigating a powder mixture with a preset molar ratio of Ca/P = 1.67, including plate-like particles, which are able to restrain shrinkage during sintering of HA-ceramics for microporosity creation. To prepare the powder mixture with a preset molar ratio of Ca/P = 1.67, the powder of HA was treated in a water solution of oxalic acid $H_2C_2O_4$ under mechanical activation conditions. We expected that the interaction of basic calcium phosphate salt ($Ca_{10}(PO_4)_6(OH)_2$, HA) with the water solution of oxalic acid $H_2C_2O_4$ will provide us the opportunity to prepare a powder mixture including brushite (calcium hydrophosphate dihydrate), $CaHPO_4{\cdot}2H_2O$, and calcium oxalate monohydrate, $CaC_2O_4{\cdot}H_2O$.

2. Materials and Methods

In order to obtain powder mixtures including calcium hydrophosphate dihydrate (brushite) $CaHPO_4{\cdot}2H_2O$ and calcium oxalate monohydrate $CaC_2O4{\cdot}H_2O$, powders of HA $Ca_{10}(PO_4)_6(OH)_2$ (CAS No. 1306-06-5, puriss. p.a. $\geq$ 90%, RiedeldeHaen, Sigma-Aldrich Laborchemikalien, 04238, lot 70080, Seelze, Germany) and oxalic acid dihydrate $H_2C_2O_4{\cdot}2H_2O$ (grade "pure," GOST 22180-76) were used. These powders were taken in a molar ratio of $Ca_{10}(PO_4)_6(OH)_2/H_2C_2O_4$ = 1:4. The following reaction (1) was used for the calculation of the quantity of starting powders.

$$Ca_{10}(PO_4)_6(OH)_2 + 4H_2C_2O_4{\cdot}2H_2O + 6H_2O = 4CaC_2O_4{\cdot}H_2O + 6CaHPO_4{\cdot}2H_2O \quad (1)$$

Oxalic acid dihydrate $H_2C_2O_4 \cdot 2H_2O$ powder measuring 5.02 g, 10.00 g of HA $Ca_{10}(PO_4)_6(OH)_2$ powder, and 55 g of grinding media (balls based on ZrO_2-ceramics) were placed in an agate vessel. Distilled water measuring 40 mL was added to the resulting mixture. The vessel was installed in a planetary mill. The treatment of HA $Ca_{10}(PO_4)_6(OH)_2$ powder in water solution of oxalic acid $H_2C_2O_4$ (1 M) was conducted for 15 min in a planetary mill (Fritch Pulverisette, Idar-Oberstein, Germany) at a rotation speed of 500 rpm. Then, the resulting suspension was placed into a porcelain cup and dried in the air for a week until the water completely evaporated.

Pre-ceramic powder compacts in the form of discs with a diameter of 12 mm and a height of 2–3 mm were made from a prepared powder mixture using a manual press (Carver Laboratory Press model C, Fred S. Carver, Inc., Wabash, IN, USA) at 100 MPa using a steel mold. Then, the samples were fired in the air in a furnace at 500 °C, 1000 °C, 1100 °C, and 1200 °C, with exposure at specified temperatures for 2 hours (the heating rate of the furnace was 5 °C/min). The mass, linear dimensions of the samples were measured before and after firing. Then, linear shrinkage and density of samples were calculated. The prepared powder mixture was additionally heat-treated at 200 °C with exposure at this temperature for 30 minutes (the heating rate of the furnace was 5 °C/min) for a better understanding of processes of transformation of phase composition of powder system under heating.

The phase composition of the powder mixture after treatment in a planetary mill and after heat treatment at 200 °C as well as ceramic samples after firing was examined by X-ray powder diffraction (XRD) (diffractometer Rigaku D/Max-2500 (Rigaku Corporation, Tokyo, Japan) with a rotating anode, a 2 Θ angle range of 2–70° with a step of 0.02° and CuKα radiation). Phase analysis was performed using the ICDD PDF2 database [32] and Match! software (https://www.crystalimpact.com/, 31 January 2022).

The prepared powder mixture after drying was examined by synchronous thermal analysis (TA), which was performed on a NETZSCH STA 449 F3 Jupiter thermal analyzer (NETZSCH, Selb, Germany) in the air at a heating rate of 10 °C/min. The mass of the sample was at least 10 mg. The composition of the gas phase formed during the heating of powder mixture was studied using a quadrupole mass spectrometer QMS 403 Quadro (NETZSCH, Selb, Germany) combined with a thermal analyzer NETZSCH STA 449 F3 Jupiter. Mass spectra (MS) were recorded for the mass numbers 18 (H_2O) and 44 (CO_2).

The powder mixtures after treatment in a planetary mill and ceramics after firing were examined by scanning electron microscopy (SEM) on a LEO SUPRA 50VP electron microscope (Carl Zeiss, Jena, Germany; auto-emission source). This investigation was carried out at an accelerating voltage of 3–20 kV in secondary electrons (SE2 detector). The surface of the samples was coated with a layer of chromium (up to 10 nm).

3. Results and Discussion

According to XRD data (Figure 1), the phase composition of powder mixture obtained as a result of the interaction of HA $Ca_{10}(PO_4)_6(OH)_2$ powder with a 1 M water solution of oxalic acid $H_2C_2O_4$ under mechanical activation condition and drying in air for a week consisted of brushite (calcium hydrophosphate dihydrate) $CaHPO_4 \cdot 2H_2O$ and calcium oxalate monohydrate $CaC_2O_4 \cdot H_2O$ in form of whewellite (PDF card 20-231) and weddellite (PDF card 17-541).

The XRD data confirmed that reaction (1) took place during treatment in planetary mill and drying of suspension. According to Match! software (https://www.crystalimpact.com/ (accessed on 30 January 2022)) phase composition of prepared powder mixture consisted of brushite $CaHPO_4 \cdot 2H_2O$ (Entry number 96-231-0527, 84.1 %) [33] and weddellite $CaC_2O_4 \cdot 2.2H_2O$ (Entry number 96-231-0999, 15.9%) [34]. Additionally, the Match! Phase Analysis Report marked 30% as unidentified peak area. The phase compositions of prepared powder mixture determined by using different programs are in good correlation. It should be noted that some quasi-crystalline phases not detected via XRD could form

during the interaction of HA $Ca_{10}(PO_4)_6(OH)_2$ powder with the water solution of oxalic acid $H_2C_2O_4$.

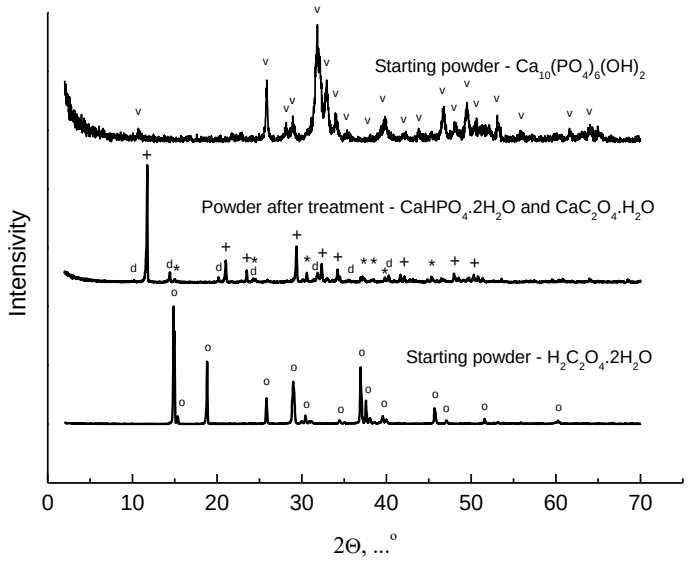

Figure 1. XRD data for starting components and resulting powder mixture: v—$Ca_{10}(PO_4)_6(OH)_2$ (PDF card 9-432); o—$H_2C_2O_4{\cdot}2H_2O$ (PDF card 14-832); +—$CaHPO_4{\cdot}2H_2O$ (PDF card 9-77); *—$CaC_2O_4{\cdot}H_2O$ (PDF card 20-231); d—$CaC_2O_4{\cdot}H_2O$ (PDF card 17-541).

Figure 2 shows a micrograph of the powder mixture obtained as a result of the interaction of HA $Ca_{10}(PO_4)_6(OH)_2$ powder with a 1 M water solution of oxalic acid $H_2C_2O_4$ under conditions of mechanical activation and drying in air for 1 week. On the micrograph, one can observe two types of particles: particles of a plate-like morphology with dimensions about 10–20 μm (Figure 2a) and particles of isometric morphology and dimensions up to 100 nm. The plate-like morphology is inherent to brushite $CaHPO_4{\cdot}2H_2O$ according to scientific literature data and our experience [35]. Thus, we could assume that particles with isometric morphology and dimensions up to 100 nm were weddellite or whewellite (calcium oxalate monohydrate) $CaC_2O_4{\cdot}H_2O$. One can observe that these isomeric particles are presented in powder as aggregates with dimensions of 500–1000 nm and as individual particles on the surface of plate-like brushite $CaHPO_4{\cdot}2H_2O$ particles (Figure 2b).

Figure 3 shows the data of synchronous thermal analysis: thermogravimetry (TG) and differential scanning calorimetry (DSC) curves for the studied powder mixture when heated from 40 °C to 1000 °C. Figure 4 shows the mass spectra of evolving gases with m/Z = 18 (H_2O) and m/Z = 44 (CO_2) resulting from the thermal decomposition of components of the powder mixture. The total mass loss of the powder mixture when heated up to 1000 °C was 33%. It should be noted that if the powder mixture was only from the product formed according to reaction (1), the total mass loss according to calculation would be 42%. This fact can additionally point out the possible presence of non-detected by means of XRD and less hydrated quasi-amorphous products formed during treatment of HA $Ca_{10}(PO_4)_6(OH)_2$ powder in a water solution of oxalic acid $H_2C_2O_4$ in the conditions of mechanical activation. There are three noticeable steps on the curve of mass loss. Mass loss at the first step is estimated at 14% (90–300 °C); at the second step, it is estimated to be 10 % (300–550 °C); and at the third step, it is estimated to be 9 % (550–750 °C).

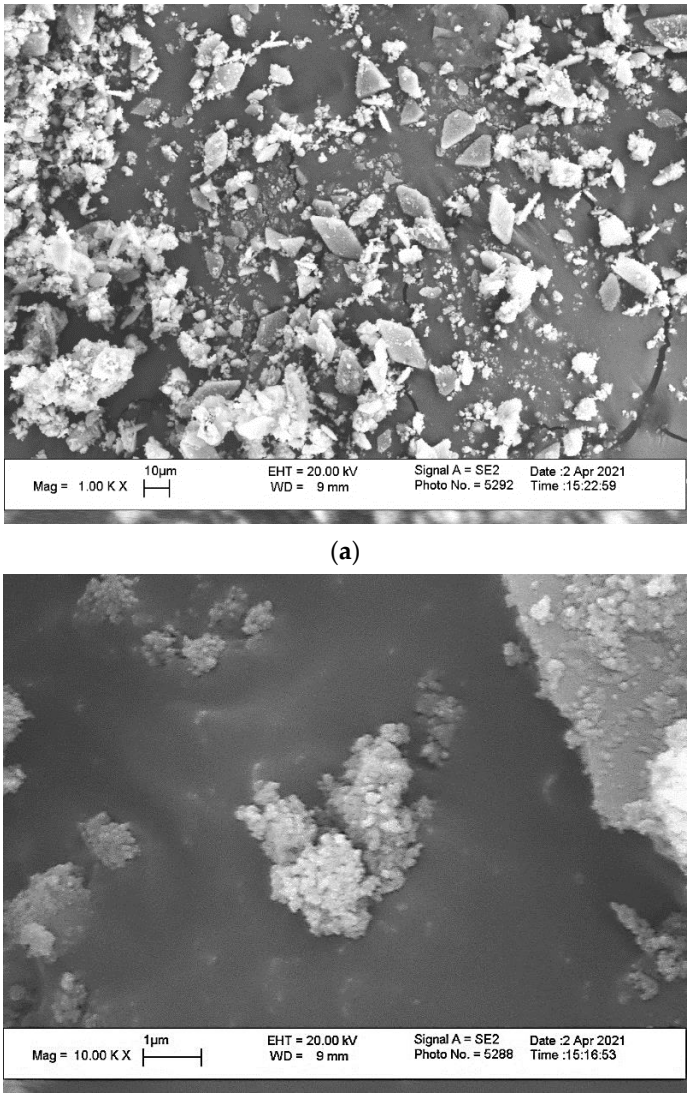

Figure 2. SEM images of the powder mixture obtained by the interaction of HA powder $Ca_{10}(PO_4)_6(OH)_2$ with a water solution of oxalic acid $H_2C_2O_4$ under mechanical activation after drying in air for a week: ×1000 (**a**) and ×10,000 (**b**).

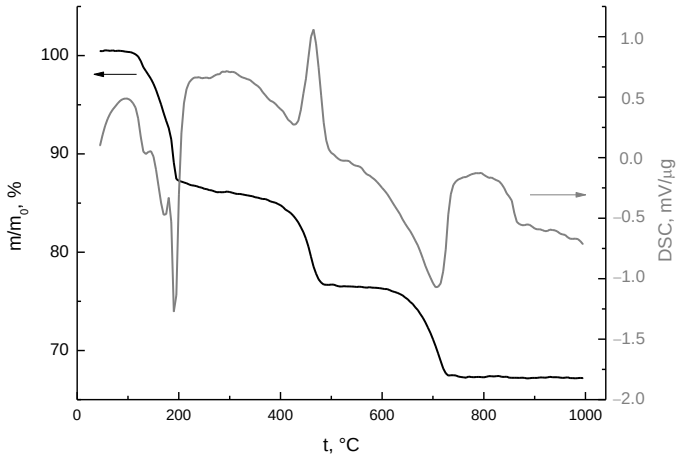

Figure 3. The results of synchronous thermal analysis (TA): thermogravimetry curves (TG, in black) and differential scanning calorimetry (DSC, in gray).

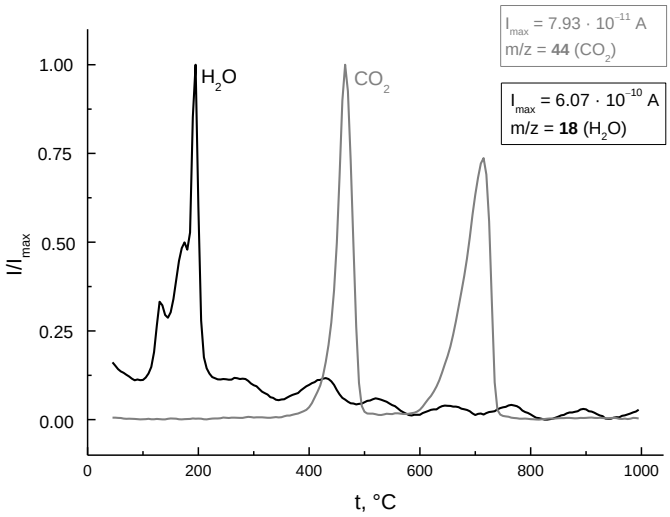

Figure 4. Mass spectra for evolving gases with m/Z=18 (in black) and m/Z=44 (in grey). Curves were normalized with respect to Imax = $6.07 \cdot 10^{-10}$ A for H_2O (m/Z = 18) and to Imax = $7.93 \cdot 10^{-11}$ A for CO_2 (m/Z = 44).

There are three endopeaks on the DSC curve in the first temperature interval (130 °C, 173 °C, and 192 °C). In the mass spectrum curve for m/Z = 18 (H_2O), in the range of 90–300 °C, one can observe three peaks at the same temperatures. The thermal decomposition of whewellite/weddellite $CaC_2O_4 \cdot H_2O$ and brushite $CaHPO_4 \cdot 2H_2O$ can take place in this range of temperatures according to reactions (2) and (3), respectively, with the formation of anhydrous calcium oxalate CaC_2O_4 and monetite $CaHPO_4$.

$$CaC_2O_4 \cdot H_2O = CaC_2O_4 + H_2O \quad (2)$$

$$CaHPO_4 \cdot 2H_2O = CaHPO_4 + 2H_2O \quad (3)$$

According to scientific literature data, the thermal decomposition of $CaC_2O_4 \cdot H_2O$ (reaction (2)) takes place at 167.9 °C [36], and thermal decomposition of brushite $CaHPO_4 \cdot 2H_2O$ takes place at 200 °C (reaction (3)) [37]. It should be noted that simultaneous presences of these two hydrated salts can influence thermal decomposition processes of each of them. And the mass loss at 130 °C can be explained by possible interaction of these two hydrated calcium salts. Moreover, this peak may reflect the process of thermal transformation of quasi-amorphous phase presence of which is possible according to XRD data. After heat treatment at 200 °C, according to XRD data (Figure 5, Table 1), the following phases were detected in the powder mixture: $CaHPO_4$, $Ca_3(PO_4)_2 \cdot xH_2O$, and $CaC_2O_4 \cdot H_2O$. The presence of $CaC_2O_4 \cdot H_2O$ in powder mixtures indicates the incompleteness of the thermal decomposition process according to reaction (2). The form of the XRD curve (Figure 5) indicates that a remarkable part of the powder mixture under investigation presents in quasi-amorphous form after heat treatment at 200 °C.

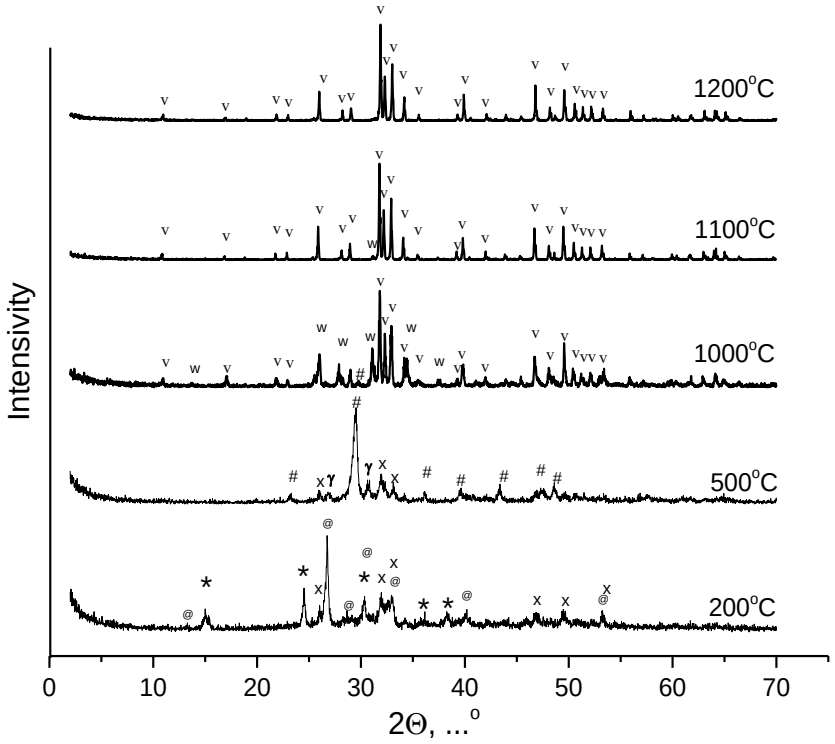

Figure 5. XRD data for powder mixture (200 °C) and ceramic samples (500 °C, 1000 °C, 1100 °C and 1200 °C) after firing: v—$Ca_{10}(PO_4)_6(OH)_2$ (PDF card 9-432); w— β-$Ca_3(PO_4)_2$ (PDF card 9-169); "#"—$CaCO_3$ (PDF card 5-586), *—$CaC_2O_4 \cdot H_2O$ (PDF card 20-231); @—$CaHPO_4$ (PDF card 9-80); x—$Ca_3(PO_4)_2 \cdot xH_2O$ (PDF card 18-303); γ — γ-$Ca_2P_2O_7$ (PDF card 17-499).

Table 1. Phase composition of powder mixtures and ceramic samples.

After Mill	200 °C	500 °C	1000 °C	1100 °C	1200 °C
$CaHPO_4 \cdot 2H_2O$	$CaHPO_4$	γ-$Ca_2P_2O_7$	$Ca_{10}(PO_4)_6(OH)_2$	$Ca_{10}(PO_4)_6(OH)_2$	$Ca_{10}(PO_4)_6(OH)_2$
non-identified phase	$Ca_3(PO_4)_2 \cdot xH_2O$	$Ca_3(PO_4)_2$ xH_2O	β-$Ca_3(PO_4)_2$	β-$Ca_3(PO_4)_2$ *	
$CaC_2O_4 \cdot H_2O$	$CaC_2O_4 \cdot H_2O$	$CaCO_3$	$CaCO_3$ *		

*—small quantity.

The second noticeable step on the curve of mass loss is in the temperature interval of 300–550 °C (Figure 3). At mass spectra for m/Z = 44 in this interval, there is a peak (465 °C) that reflects CO_2 evolving. The thermal decomposition of anhydrous calcium oxalate CaC_2O_4 with the formation of calcium carbonate $CaCO_3$ takes place with the release of heat (DSC curve, Figure 3) according to reaction (4) [36].

$$CaC_2O_4 + 1/2O_2 = CaCO_3 + CO_2 \quad (4)$$

The grey color of the samples after firing at 500 °C provides us with the opportunity to form a conclusion about the presence of some quantity of amorphous carbon in the powder compact. In the temperature range from 400 °C to 450 °C, monetite $CaHPO_4$ undergoes dehydration with the formation of calcium diphosphate γ-$Ca_2P_2O_7$ (reaction (5), which is confirmed by a peak (425 °C) on the mass spectrum curve (Figure 4, m/Z = 18).

$$2CaHPO_4 = \gamma\text{-}Ca_2P_2O_7 + H_2O \quad (5)$$

XRD data after heat treatment at 500 °C (Figure 5, Table 1) confirm the presence of calcium carbonate $CaCO_3$ in the form of calcite and γ-calcium pyrophosphate γ-$Ca_2P_2O_7$ in the phase composition of samples. The simultaneous presence at powder system of calcium

carbonate $CaCO_3$ and calcium pyrophosphate $Ca_2P_2O_7$ makes it possible for the formation of tricalcium phosphate $Ca_3(PO_4)_2$ or hydroxyapatite $Ca_{10}(PO_4)_6(OH)_2$ according to reactions (6) and (7). Tricalcium phosphate $Ca_3(PO_4)_2$ can form due to thermal decomposition of hydrated tricalcium phosphate $Ca_3(PO_4)_2$ xH_2O (analog of Ca-deficient HA–$Ca_9(HPO_4)(PO_4)_5(OH)$) (reactions (8) and (9)). Moreover, hydroxyapatite $Ca_{10}(PO_4)_6(OH)_2$ can form from tricalcium phosphate $Ca_3(PO_4)_2$ and calcium carbonate $CaCO_3$ according to reaction (10).

$$CaCO_3 + Ca_2P_2O_7 = Ca_3(PO_4)_2 + CO_2 \quad (6)$$

$$4CaCO_3 + 3Ca_2P_2O_7 + H_2O = Ca_{10}(PO_4)_6(OH)_2 + 4CO_2 \quad (7)$$

$$Ca_3(PO_4)_2\ xH_2O = Ca_3(PO_4)_2 + xH_2O \quad (8)$$

$$Ca_9(HPO_4)(PO_4)_5(OH) = 3Ca_3(PO_4)_2 + H_2O \quad (9)$$

$$3Ca_3(PO_4)_2 + CaCO_3 + H_2O = Ca_{10}(PO_4)_6(OH)_2 + CO_2 \quad (10)$$

Reactions (6), (7), and (10) can explain CO_2 evolving (peak at 715 °C, Figure 4) in the third noticeable step at the mass loss curve in the interval 550–750 °C (Figure 3). As one can observe, no mass changes were detected during heating in the interval of 750–1000 °C in the TG curve.

Figure 5 shows XRD data of powder mixture after heat treatment at 200 °C and ceramic samples based on powder mixtures prepared from the powder of HA $Ca_{10}(PO_4)_6(OH)_2$ and oxalic acid dihydrate $H_2C_2O_4{\cdot}2H_2O$ after firing at 500 °C, 1000 °C, 1100 °C, and 1200 °C. Table 1 briefly summarizes phase transformations in powder systems under investigation from the starting powder mixture ($CaHPO_4{\cdot}2H_2O$ and $CaC_2O_4{\cdot}H_2O$; non-identified phase quasi-amorphous phase) to final monophase HA ($Ca_{10}(PO_4)_6(OH)_2$) ceramics. The phase composition of ceramics after firing at 1000 °C included HA ($Ca_{10}(PO_4)_6(OH)_2$), β-tricalcium phosphate β-$Ca_3(PO_4)_2$, and a small quantity of calcite $CaCO_3$. The presence of β-tricalcium phosphate β-$Ca_3(PO_4)_2$ after firing at 1000 °C can be explained with the possibility of reaction (6) in the 550–770 °C interval and reactions (8), (9) and (10), describing the transformation of hydrated tricalcium phosphates $Ca_3(PO_4)_2$ xH_2O (as it was described in PDF card 18-303) or Ca-deficient hydroxyapatite $Ca_9(HPO_4)(PO_4)_5(OH)$ relative to β-tricalcium phosphate β-$Ca_3(PO_4)_2$, which is possible in the 650–800 °C interval [38,39].

The phase composition of ceramics after firing at 1100 °C included HA ($Ca_{10}(PO_4)_6$-$(OH)_2$) and a small quantity of β-tricalcium phosphate β-$Ca_3(PO_4)_2$. Finally, the phase composition of ceramics after firing at 1200 °C included phase-HA ($Ca_{10}(PO_4)_6(OH)_2$) only.

XRD data of samples after heat treatment at different temperatures show that the formation of single-phase HA-ceramics from multi-component homogenized powder mixture took place as a complicated sequence of different heterogeneous reactions, including thermal decomposition reactions and solid-state reactions. As it is known from the scientific literature, heterophase reactions can take place during firing and accompany the sintering process of HA-ceramics [40,41]. The investigation presented in this article emphasizes the importance of the preset Ca/P = 1.67 molar ratio in the starting powder mixture when preparing ceramics based on HA. Presetting Ca/P = 1.67 in the starting powder mixture in this work was guaranteed both by the high quality HA powder used and by the preparation of the powder mixture via acid–base reactions in the mechanical activation condition. This method excludes changes in the preset Ca/P molar ratio due to differences in solubility of the starting components or influences of pH on preferability for the formation of one or more other phases, as it would be possible in the case of precipitation of calcium phosphate powders from solutions.

A micrograph of the surface of the ceramic sample based on the powder mixture including brushite (calcium hydrophosphate dihydrate) $CaHPO_4{\cdot}2H_2O$ and calcium oxalate monohydrate $CaC_2O_4{\cdot}H_2O$ in the form of whewellite and weddellite after firing at 1200 °C is presented at Figure 6. The microstructure of the ceramic sample fired at 1200 °C comprised polycrystalline plate-like particles with dimensions 5–15 μm, arched groups of particles 0.5–2 μm and two types of pores with dimensions about 10 and 1–2 μm.

Obviously, the microstructure of HA-ceramics inherits the microstructure of the starting powder mixture. It can be assumed that the formation of the phase of HA was realized both on the surfaces of nanosized particles of calcium oxalate/calcium carbonate and on the surfaces of microsized plate-like particles of brushite/monetite/calcium pyrophosphate.

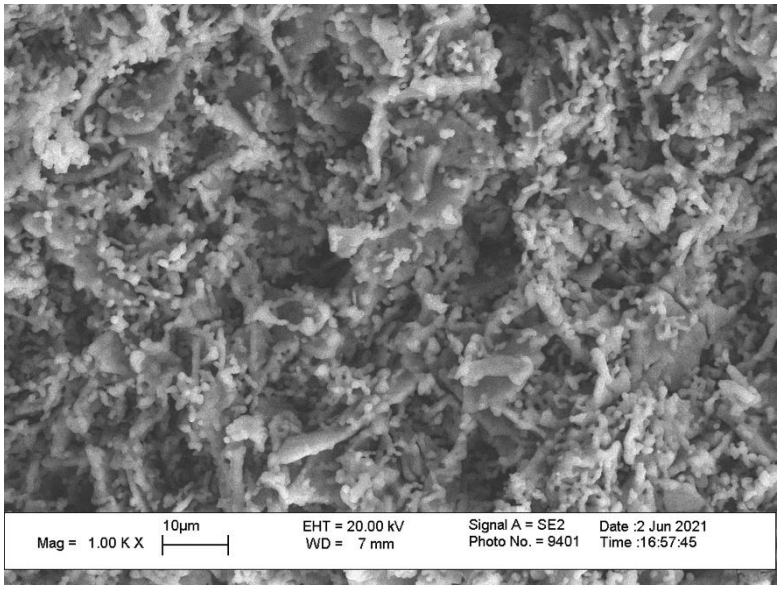

Figure 6. Micrograph of the surface of the ceramic sample based on powder mixture including brushite (calcium hydrophosphate dihydrate) $CaHPO_4 \cdot 2H_2O$, calcium oxalate monohydrate $CaC_2O_4 \cdot H_2O$ in form of whewellite and weddellite and non-identified phase after firing at 1200 °C.

Apparent density (g/cm^3) and relative diameter (D/D_0, %) of ceramic samples after firing at different temperatures are presented at Figure 7. Linear shrinkage increased very slowly from 1% at 500 °C up to 2.7% at 1100 °C and reach the maximum of 7 % at 1200 °C. Liner shrinkage of HA-ceramics based on uniform synthetic HA powders consisted of isometric particles that could reach about 20% [42] or even more than 20% [43]. Ceramic samples prepared from the powder mixture ($CaHPO_4 \cdot 2H_2O$ and $CaC_2O_4 \cdot H_2O$; non-identified quasi-amorphous phase) had the maximum density of 1.25 g/cm^3 (~40% relatively theoretical density of HA) after firing at 1200 °C. Therefore, the microstructure of HA-ceramics (Figure 6), data of apparent density, and relative diameter after firing (Figure 7) confirm the possibility to create microporosity via the utilization of powder mixtures with plate-like particle restraining shrinkage during sintering.

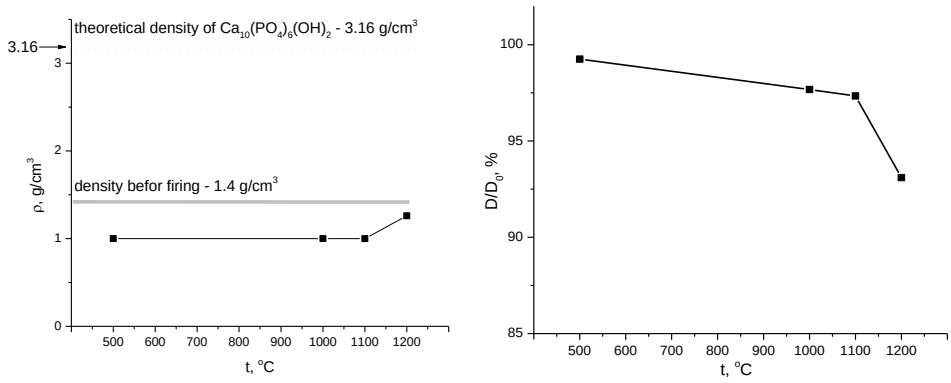

Figure 7. Apparent density (g/cm^3) and relative diameter (D/D_0, %) of ceramic samples based on powder mixture ($CaHPO_4 \cdot 2H_2O$ and $CaC_2O_4 \cdot H_2O$; non-identified quasi-amorphous phase) after firing at different temperatures.

4. Conclusions

A powder mixture with a given molar ratio Ca/P = 1.67 consisting of plate-like particles of brushite (calcium hydrophosphate dihydrate) $CaHPO_4 \cdot 2H_2O$; nanosized isometric particles of calcium oxalate monohydrate $CaC_2O_4 \cdot H_2O$ in form of whewellite and weddellite; and some quantity of non-identified quasi-amorphous phase was obtained as a result of the interaction of HA powder $Ca_{10}(PO_4)_6(OH)_2$ with an aqueous solution of oxalic acid $H_2C_2O_4$ at a molar ratio of $Ca_{10}(PO_4)_6(OH)_2/H_2C_2O_4$ = 1:4 under mechanical activation conditions. This powder was used for the creation of microporous monophase HA $Ca_{10}(PO_4)_6(OH)_2$ ceramics. Components of prepared powder mixture with preset Ca/P=1.67 molar ratio take part both in the sequences of thermal transformations, such as dehydration and decomposition, and then in sequences of heterophase reactions, resulting in a final and target phase composition of ceramics presented by HA $Ca_{10}(PO_4)_6(OH)_2$ It was shown that plate-like particles presented in the powder used for ceramic creation can restrain sintering processes and provide the formation of microporosity of HA $Ca_{10}(PO_4)_6(OH)_2$ ceramics.

Author Contributions: Conceptualization, T.S. (Tatiana Safronova); methodology, T.S. (Tatiana Safronova); investigation, S.C., T.S. (Tatiana Shatalova), Y.F. and T.S. (Tatiana Safronova); writing—original draft preparation, S.C. and T.S. (Tatiana Safronova); writing—review and editing, T.S. (Tatiana Safronova); visualization, S.C., T.S. (Tatiana Shatalova), Y.F. and T.S. (Tatiana Safronova); supervision, T.S. (Tatiana Safronova); project administration, T.S. (Tatiana Safronova); funding acquisition, T.S. (Tatiana Safronova). All authors have read and agreed to the published version of the manuscript.

Funding: This research was funded by Russian Foundation for Basic Research, grant number 18-29-11079.

Institutional Review Board Statement: Not applicable.

Informed Consent Statement: Not applicable.

Data Availability Statement: Not applicable.

Acknowledgments: The research was carried out using the equipment of MSU Shared Research Equipment Center "Technologies for obtaining new nanostructured materials and their complex study" and purchased by MSU in the frame of the Equipment Renovation Program (National Project "Science") and in the frame of the MSU Program of Development.

Conflicts of Interest: The authors declare no conflict of interest.

References

1. Huang, J.; Best, S.M. Ceramic biomaterials for tissue engineering. In *Tissue Engineering Using Ceramics and Polymers*, 3rd ed.; Boccaccini, A.R., Ma, P.X., Liverani, L., Eds.; Woodhead Publishing: Cambridge, UK, 2022; Chapter 1; pp. 3–40. ISBN 9780128205082. [CrossRef]
2. Matveichuk, I.V.; Rozanov, V.V.; Litvinov, Y.Y. Biophysical properties of bone tissue for biomedical applications. *Al'manakh Klinich. Med.* **2016**, *44*, 193–202. [CrossRef]
3. Quelch, K.J.; Melick, R.A.; Bingham, P.J.; Mercuri, S.M. Chemical composition of human bone. *Arch. Oral Biol.* **1983**, *28*, 665–674. [CrossRef]
4. Simske, S.J.; Ayers, R.A.; Bateman, T.A. Porous materials for bone engineering. *Mater. Sci. Forum.* **1997**, *250*, 151–182. [CrossRef]
5. Yoshikawa, H.; Myoui, A. Bone tissue engineering with porous hydroxyapatite ceramics. *J. Artif. Organs* **2005**, *8*, 131–136. [CrossRef] [PubMed]
6. Jones, J.R.; Lee, P.D.; Hench, L.L. Hierarchical porous materials for tissue engineering. *Philos. Trans. R. Soc. A Math. Phys. Eng. Sci.* **2006**, *364*, 263–281. [CrossRef]
7. Putlyaev, V.I.; Safronova, T.V. Chemical Transformations of Calcium Phosphates during Production of Ceramic Materials on Their Basis. *Inorg. Mater.* **2019**, *55*, 1328–1341. [CrossRef]
8. Nikolenko, M.V.; Vasylenko, K.V.; Myrhorodska, V.D.; Kostyniuk, A.; Likozar, B. Synthesis of calcium orthophosphates by chemical precipitation in aqueous solutions: The effect of the acidity, Ca/P molar ratio, and temperature on the phase composition and solubility of precipitates. *Processes* **2020**, *8*, 1009. [CrossRef]
9. Yoon, S.Y.; Park, Y.M.; Park, S.S.; Stevens, R.; Park, H.C. Synthesis of hydroxyapatite whiskers by hydrolysis of α-tricalcium phosphate using microwave heating. *Mater. Chem. Phys.* **2005**, *91*, 48–53. [CrossRef]

10. Earl, J.S.; Wood, D.J.; Milne, S.J. Hydrothermal synthesis of hydroxyapatite. In *Journal of Physics: Conference Series*; IOP Publishing: Bristol, UK, 2006; Volume 26, pp. 268–271. [CrossRef]
11. Rabiee, S.M.; Moztarzadeh, F.; Solati-Hashjin, M. Synthesis and characterization of hydroxyapatite cement. *J. Mol. Struct.* **2010**, *969*, 172–175. [CrossRef]
12. Javadinejad, H.R.; Ebrahimi-Kahrizsangi, R. Thermal and kinetic study of hydroxyapatite formation by solid-state reaction. *Int. J. Chem. Kinet.* **2021**, *53*, 583–595. [CrossRef]
13. Pu'ad, N.M.; Haq, R.A.; Noh, H.M.; Abdullah, H.Z.; Idris, M.I.; Lee, T.C. Synthesis method of hydroxyapatite: A review. *Mater. Today Proc.* **2019**, *29*, 233–239. [CrossRef]
14. Safronova, T.V.; Putlyaev, V.I.; Ivanov, V.K.; Knot'ko, A.V.; Shatalova, T.B. Powders Mixtures Based on Ammonium Pyrophosphate and Calcium Carbonate for Preparation of Biocompatible Porous Ceramic in the $CaO–P_2O_5$ System. *Refract. Ind. Ceram.* **2016**, *56*, 502–509. [CrossRef]
15. Taş, A.C. Molten salt synthesis of calcium hydroxyapatite whiskers. *J. Am. Ceram. Soc.* **2001**, *84*, 295–300. [CrossRef]
16. Tan, J.; Liu, Y.; Gong, J.; Jin, X.; Cheng, C.; Zhang, R.; Chen, M. Non-aqueous liquid crystals of hydroxyapatite nanorods. *Acta Biomater.* **2020**, *116*, 383–390. [CrossRef] [PubMed]
17. Hassan, M.N.; Mahmoud, M.M.; El-Fattah, A.A.; Kandil, S. Microwave-assisted preparation of Nano-hydroxyapatite for bone substitutes. *Ceram. Int.* **2016**, *42*, 3725–3744. [CrossRef]
18. Rhee, S.H. Synthesis of hydroxyapatite via mechanochemical treatment. *Biomaterials* **2002**, *23*, 1147–1152. [CrossRef]
19. Kojima, Y.; Kitazawa, K.; Nishimiya, N. Synthesis of nano-sized hydroxyapatite by ultrasound irradiation. In *Journal of Physics: Conference Series*; IOP Publishing: Bristol, UK, 2012; Volume 339, p. 012001. [CrossRef]
20. Batista, H.A.; Silva, F.N.; Lisboa, H.M.; Costa, A.C.F.M. Modeling and optimization of combustion synthesis for hydroxyapatite production. *Ceram. Int.* **2020**, *46*, 11638–11646. [CrossRef]
21. DileepKumar, V.G.; Sridhar, M.S.; Aramwit, P.; Krut'ko, V.K.; Musskaya, O.N.; Glazov, I.E.; Reddy, N. A review on the synthesis and properties of hydroxyapatite for biomedical applications. *J. Biomater. Sci. Polym. Ed.* **2022**, *33*, 229–261. [CrossRef]
22. Rial, R.; González-Durruthy, M.; Liu, Z.; Ruso, J.M. Advanced materials based on nanosized hydroxyapatite. *Molecules* **2021**, *26*, 3190. [CrossRef]
23. Safronova, T.V.; Putlyaev, V.I. Powder systems for calcium phosphate ceramics. *Inorg. Mater.* **2017**, *53*, 17–26. [CrossRef]
24. Safronova, T.V.; Putlyaev, V.I.; Shekhirev, M.A.; Kuznetsov, A.V. Disperse systems in calcium hydroxyapatite ceramics technology. *Glass Ceram.* **2007**, *64*, 22–26. [CrossRef]
25. Layrolle, P.; Ito, A.; Tateishi, T. Sol-gel synthesis of amorphous calcium phosphate and sintering into microporous hydroxyapatite bioceramics. *J. Am. Ceram. Soc.* **1998**, *81*, 1421–1428. [CrossRef]
26. Studart, A.R.; Gonzenbach, U.T.; Tervoort, E.; Gauckler, L.J. Processing routes to macroporous ceramics: A review. *J. Am. Ceram. Soc.* **2006**, *89*, 1771–1789. [CrossRef]
27. Iwamoto, T.; Hieda, Y.; Kogai, Y. Effects of molecular weight on macropore sizes and characterization of porous hydroxyapatite ceramics fabricated using polyethylene glycol: Mechanisms to generate macropores and tune their sizes. *Mater. Today Chem.* **2021**, *20*, 100421. [CrossRef]
28. Seesala, V.S.; Rajasekaran, R.; Dutta, A.; Vaidya, P.V.; Dhara, S. Dense-porous multilayer ceramics by green shaping and salt leaching. *Open Ceram.* **2021**, *5*, 100084. [CrossRef]
29. Neeraj, V.S.; Wilson, P.; Vijayan, S.; Prabhakaran, K. Porous ceramics with a duplex pore structure by compression molding of alumina-NaCl paste in molten sucrose. *Ceram. Int.* **2017**, *43*, 14107–14113. [CrossRef]
30. Barinov, S.M. Calcium phosphate-based ceramic and composite materials for medicine. *Russ. Chem. Rev.* **2010**, *79*, 13–29. [CrossRef]
31. Beletskii, B.I.; Shumskii, V.I.; Nikitin, A.A.; Vlasova, E.B. Biocomposite calcium-phosphate materials used in osteoplastic surgery. *Glass Ceram.* **2000**, *57*, 322–325. [CrossRef]
32. ICDD. PDF-4+ 2010 (Database), Ed. by Dr. Soorya Kabekkodu (International Centre for Diffraction Data, Newtown Square, PA, USA, 2010). Available online: https://www.icdd.com/pdf-2/ (accessed on 30 January 2022).
33. Beevers, C.A. The crystal structure of dicalcium phosphate dihydrate, $CaHPO_4·2H_2O$. *Acta Crystallogr.* **1958**, *11*, 273–277. [CrossRef]
34. Sterling, C. Crystal structure analysis of weddellite, $CaC_2O_4·(2+x)H_2O$. *Acta Crystallogr.* **1965**, *18*, 917–921. [CrossRef]
35. Safronova, T.V.; Shatalova, T.B.; Tikhonova, S.A.; Filippov, Y.Y.; Krut'ko, V.K.; Musskaya, O.N.; Kononenko, N.E. Synthesis of Calcium Pyrophosphate Powders from Phosphoric Acid and Calcium Carbonate. *Inorg. Mater. Appl. Res.* **2021**, *12*, 986–992. [CrossRef]
36. Chang, H.; Huang, P.J. Thermal Decomposition of $CaC_2O_4·H_2O$ Studied by Thermo-Raman Spectroscopy with TGA/DTA. *Anal. Chem.* **1997**, *69*, 1485–1491. [CrossRef]
37. Dosen, A.; Giese, R.F. Thermal decomposition of brushite, $CaHPO_4·2H_2O$ to monetite CaHPO4 and the formation of an amorphous phase. *Am. Miner.* **2011**, *96*, 368–373. [CrossRef]
38. Safronova, T.V.; Putlyaev, V.I.; Avramenko, O.A.; Shekhirev, M.A.; Veresov, A.G. Ca-deficient hydroxyapatite powder for producing tricalcium phosphate based ceramics. *Glass Ceram.* **2011**, *68*, 28–32. [CrossRef]

39. Safronova, T.; Putlayev, V.; Filippov, Y.; Shatalova, T.; Karpushkin, E.; Larionov, D.; Kazakova, G.; Shakhtarin, Y. Calcium phosphate powder synthesized from calcium acetate and ammonium hydrophosphate for bioceramics application. *Ceramics* **2018**, *1*, 375–392. [CrossRef]
40. Champion, E. Sintering of calcium phosphate bioceramics. *Acta Biomater.* **2013**, *9*, 5855–5875. [CrossRef]
41. Mitsionis, A.I.; Vaimakis, T.C.; Trapalis, C.C. The effect of citric acid on the sintering of calcium phosphate bioceramics. *Ceram. Int.* **2010**, *36*, 623–634. [CrossRef]
42. Safronova, T.V.; Shekhirev, M.A.; Putlyaev, V.I.; Tret'yakov, Y.D. Hydroxyapatite-based ceramic materials prepared using solutions of different concentrations. *Inorg. Mater.* **2007**, *43*, 901–909. [CrossRef]
43. Raynaud, S.; Champion, E.; Bernache-Assollant, D. Calcium phosphate apatites with variable Ca/P atomic ratio II. Calcination and sintering. *Biomaterials* **2002**, *23*, 1073–1080. [CrossRef]